First Quarterly Progress Report for the Department of Natural Resources Groundwater Project

Michael Arndt
Radiochemistry Unit, Wisconsin State Laboratory of Hygiene

Abstract. This report discusses progress made in the understanding of some of the factors affecting the gross alpha measurement. It is clear that groundwater samples that have substantial Ra-228 activity also have substantial Ra-224 activity, although analysis of water samples for Ra-224 is rarely performed and is not performed in this study. To a first approximation, the activity of Ra-224 will be considered to be equal to the activity of Ra-228. Both Ra-224 and Ra-226 decay into a series of radioactive progeny, some of which are alpha emitters. The activities of these progeny are almost never measured due to their short half-lives, but the levels of these progeny radionuclides are readily calculated once the activities of the parent species, Ra-224 and Ra-226, are known. This report also discusses progress made in the development of a model to quantitatively account for the gross alpha measurement.

Introduction. The purpose of this study is twofold: (1) to analyze groundwater samples from various Wisconsin aquifers, which historically have high gross alpha activities, for the radionuclides Ra-226, Ra-228, U-234, U-235, U-238, Th-228, Th-230, Th-232, and Po-210 and (2) to quantitatively correlate the activities of these radionuclides to the measured gross alpha activity of the groundwater samples. In the past some method development had been done on the analyses for the thorium isotopes and for Po-210. This report discusses progress made in the understanding of the some of the factors affecting the gross alpha measurement and progress made in the development of a model to quantitatively account for the gross alpha measurement.

The gross alpha measurement was developed to obtain an estimate of the total alpha activity in a sample of water. In this method a small volume (50 to 100 mL) of the acidified water sample is reduced in volume by evaporation. The sample is placed in a planchet where it is reduced to dryness, leaving a solid film that contains the nonvolatile radionuclides of the water sample. The planchet is heated to a dull red glow. This causes the conversion of some hygroscopic compounds like $SiO_2 \cdot H_2O$ to decompose into non-hygroscopic compounds like SiO_2. This also reduces the mass of the solid film by decomposing some of the nitrate compounds in the solids to the corresponding oxides. (Some nitrates, like $Ca(NO_3)_2$ and $Mg(NO_3)_2$, probably decompose completely; other nitrates, like $NaNO_3$ and KNO_3, probable only decompose partially, if at all.) The alpha particle emission rate from the resulting solid film in the planchet is measured using a gas proportional detector. The purpose of decomposing the nitrate compounds is to reduce the mass of the solid film in the planchet. Excessively large amounts of solids adversely affect the alpha-particle signal. As the film mass is increased, the number of alpha particles that are absorbed in the film before reaching the detector increases. This phenomenon is often referred to as self-absorption. In practice, for a five-centimeter-diameter planchet the upper limit for the film mass is about 100 mg.

Several analytical tests are routinely performed on water samples to determine the activities of specific alpha-emitting radionuclides. These tests are the determination of the activity of Ra-226, the activity of Rn-222, and the total uranium activity, i.e., the combined activities of U-234, U-235, and U-238. Since Rn-222 is volatile, its activity in the solid film immediately after flaming is virtually zero. Consequently, people often assume that the gross alpha activity is equal to the sum of the measured activities of Ra-226 and total uranium. Such an assumption is erroneous for several reasons.

First, whenever Ra-228 is present in a water source, its third-generation progeny, Ra-224, is undoubtedly present. This decay sequence form Ra-228 to Ra-224 is shown below

$$^{228}\mathrm{Ra} \xrightarrow{b} {}^{228}\mathrm{Ac} \xrightarrow{a} {}^{228}\mathrm{Th} \xrightarrow{a} {}^{224}\mathrm{Ra}\ .$$

Because thorium is highly insoluble, it is never present to a significant extent in aquifer water. Ra-224 on the other hand has the same chemistry as Ra-228, and once formed from Th-228, readily goes into solution

under the same conditions that would cause Ra-228 to go into solution. In fact, there is recent experiment evidence that correlates the presence of Ra-224 with Ra-228.

Second, as is shown below,

$$^{226}\mathrm{Ra} \xrightarrow{a} {}^{222}\mathrm{Rn} \xrightarrow{a} {}^{218}\mathrm{Po} \xrightarrow{a} {}^{214}\mathrm{Pb} \xrightarrow{b} {}^{214}\mathrm{Bi} \xrightarrow{b} {}^{214}\mathrm{Po} \xrightarrow{a} {}^{210}\mathrm{Pb}\ ,$$

Ra-226 decays into a series of radionuclides some of which are alpha emitters. Since the half-life of Ra-226 is quite long, 1622 years, over ordinary time scales its decay results in the formation of Rn-222 at a nearly constant rate. Although Rn-222 is volatile, it becomes trapped when formed in the solid film. In turn, Rn-222 decays with a half-life of 3.6 days. The four successive progeny of Rn-222—Po-218, Pb-214, Bi-214, and Po-214—decay one into the other quite quickly. Thus, in a relatively short period of time Ra-226 gives rise to three other alpha emitters. In fact, over a period of days to weeks the activities of the three alpha emitters Rn-222, Po-218, and Po-214 increase, as their populations build, and the activity of each of the alpha emitters approaches quite closely the activity of their parent, Ra-226. This is a well established phenomenon known as secular equilibrium. Consequently, with time, the activity of Ra-226 is amplified by up to a factor of four due to itself and its three alpha emitting progeny. The activities of the two polonium isotopes are never measured in a routine analysis because of their exceedingly short half-lives.

Like Ra-226, Ra-224 gives rise to a series of alpha-emitting radionuclides. This decay sequence it shown below

$$^{224}\mathrm{Ra} \xrightarrow{a} {}^{220}\mathrm{Rn} \xrightarrow{a} {}^{216}\mathrm{Po} \xrightarrow{a} {}^{212}\mathrm{Pb} \xrightarrow{b} {}^{212}\mathrm{Bi} \rightarrow \left\{ \begin{array}{l} \xrightarrow{b} {}^{212}\mathrm{Po} \xrightarrow{a} \\ \xrightarrow{a} {}^{208}\mathrm{Tl} \xrightarrow{b} \end{array} \right\} \rightarrow {}^{208}\mathrm{Pb}\ ,$$

Ra-224 decays away with a half-life of about 3.4 days, so that it does not produce is progeny at a constant rate like Ra-226. Although the situation is somewhat more complicated than that for Ra-226, it is clear that the apparent activity of Ra-224 is amplified by the decay of its progeny. The amount of this amplification is readily determined using the Bateman equations, which are the solution of the set of ordinary linear differential equations that describe the decay of a series of radionuclides.

Third, gross alpha measurements are made on gas proportion counters. The signal obtained from the film depends on the mass and geometry of the film, and the design of the gas proportional counter. A typical gas proportional counter, used in many radiochemistry laboratories, is known as a pancake-style gas proportional counter. Such a counter along with the sample planchet is illustrated schematically in Figure 1. An alpha particle that results from the decay of a radionuclide originates within the volume of the film. In order to cause a pulse in the detector, the trajectory of the alpha particle must be such that it enters the active region of the detector, which in this case is the volume of the detector filled with P-10 gas (a mixture of 10% methane and 80% Argon). The alpha particle ionizes molecules of the P-10 gas, and the electrons created are attracted to the anode wire where the electron current is amplified (by a phenomenon known as a Townsend avalanche) and collected. Thus, an alpha particle that reaches the active region of the detector causes an electronic pulse. These electronic pulses are counted over a period of time to determine the rate at which alpha particles enter the active region of the detector. To a first approximation, every alpha particle that enters the active region of the detector with sufficient energy causes a pulse in the detector.

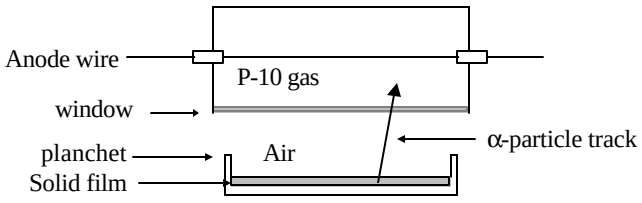

Figure 1. Schematic of sample and pancake-style gas proportional counter.

An alpha particle has a relatively well-defined range in matter. The more matter that an alpha particle must traverse in going through the solid film, the air, and the entrance window of the detector, the less energy the alpha particle has upon reaching the active region of the detector. If the alpha particle traverses too much matter, it will not reach the detector. Obviously, the more energetic that an alpha particle is, the more matter it can traverse and still reach the active region of the detector. For a given energy there is a maximum depth within the film from which an alpha particle can be emitted and still reach the detector. This depth increases with the energy of the alpha particle. This effect is illustrated in Figure 2. Consequently, the more energetic the alpha particle of a radionuclide, the more alpha particles of the radionuclide reach the active region of the detector. For a given radionuclide the fraction of the emitted alpha particles that cause a pulse in the detector is called the efficiency of the detector for that particular radionuclide; i.e.,

$$\text{detector efficiency for the } i\text{th radionuclide} = \frac{\text{pulse count in the detector due to the } i\text{th radionculide}}{\text{activity of the } i\text{th radionuclide in the film}} . \quad (1)$$

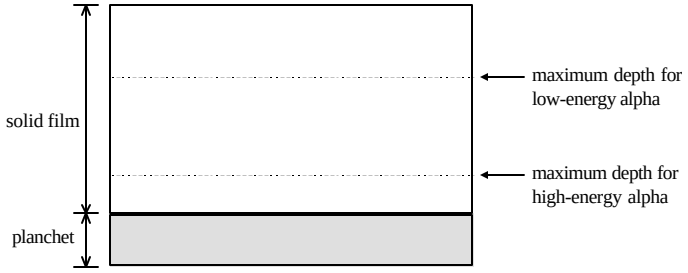

Figure 2. Schematic diagram showing the maximum depth from which an alpha particle can be emitted from Ra-226 or from Po-214 and still reach the active volume of the detector.

Radionuclides emit alpha particles with well-defined energies. Usually for a particular nuclide there is one or two alpha-particle energies that account for nearly all of the alpha particles emitted by that radionuclide. In general, the shorter the half-life of a radionuclide, the more energetic are its alpha particles. The detector is normally calibrated with an alpha emitter having a relatively long half-life, most commonly Th-230 or Am-241. The short-lived progeny of Ra-224 and Ra-226 have alpha-particle energies that far exceed the energies of the common calibration standards. Consequently, the detector efficiencies for these short-lived radionuclides are greater than that of the calibration standard. In the gross alpha method it is, in effect, assumed that the efficiency of all of the alpha emitting radionuclides is the same as the efficiency of the radionuclide used as the calibration standard. It is easy to see that such an assumption will tend to cause one to overestimate the amount of alpha activity in the film. If Equation (1) is solved for the activity of *i*th radionuclide in the film, and if it is assumed that the detector efficiency for *i*th radionuclide is equal to the detector efficiency of the calibration standard, then one obtains

$$\text{activity of the } i\text{th radionuclide in the film} = \frac{\text{pulse count in the detector due to the } i\text{th radionculide}}{\text{detector efficiency for the calibration standard}} .$$

Since, in actual fact, the detector efficiency for the calibration standard is less than the detector efficiency for *i*th radionuclide, from Equation (2), it is seen that one is actually overestimating the activity of *i*th radionuclide in the film. Up to a point, as the mass of the film is increased, the disparity between the detector efficiencies for *i*th radionuclide and the calibration standard increase. Thus, the disparity between the gross alpha activity and the actual alpha activity increases with film mass. It should be noted that most ground water samples having a high radiumactivity usually have a high level of dissolved solids. Some of the aqueous cations adsorb onto the surfaces of solids displacing the radium, causing the radium to go into

solution. This is known as the common ion effect. Thus, the gross alpha activity in samples with high radium levels is often further elevated because of the high level of dissolved solids.

The detector design also has an effect on the gross alpha activity. Increasing the thickness of the air layer and the detector entrance window places more matter between the emitted alpha particle and the active region of the detector, and, therefore, increases the difference between the gross alpha activity and the actual alpha activity.

There are two other complicating factors affecting the gross alpha activity: the solid film often covers part of the vertical wall of the planchet, and the film usually develops in such a way that it is not uniform. Quite often the film tends to form in such a way that it is composed of several relatively thick regions separated from one another by a relatively thin film. As is discussed below, the effect of the presence of these thick regions on the gross alpha signal can be to enhance it or to reduce it.

In summary, the measured gross alpha activity cannot be expected to be equal to the sum of the Ra-226 activity and the total uranium activity. In general, the presence of Ra-224 cannot be neglected when the water sample contains substantial amounts of Ra-228, unless the water sample is stored until the Ra-224 activity decays to an insignificant amount. To a first approximation, since Ra-224 is in secular equilibrium with Ra-228, it is assumed that the activity of Ra-224 is equal to the activity of Ra-228. Moreover, both Ra-224 and Ra-226 give rise to a series of alpha-emitting progeny, whose activity must be taken into account when assessing the gross alpha activity. The activities of the progeny are readily determined using the Bateman equations. Since the Ra-224 is decaying and its progeny are decaying and the progeny of Ra-224 are growing in, it is clear that, in general, the value of the gross alpha activity changes with time. Depending on the relative activities of Ra-224 and Ra-226, it is possible for the gross alpha activity to increase or decrease with time. Finally, factors like film mass and instrument parameters such as the thickness of the air layer and the entrance window of the detector tend to accentuate the contribution of the short-lived progeny of Ra-224 and Ra-224. Consequently, in order to understand the gross alpha measurement one must be able to calculate the detector efficiencies for all radionuclides present in the film. An outline of these calculations and some results are given in the next section.

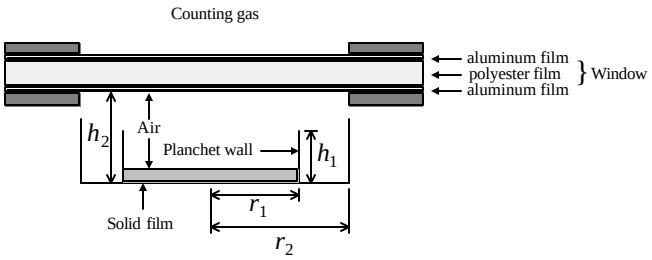

Figure 3. Schematic of sample and gas proportional counter. The sample consists of a solid film in the bottom of a planchet. The window is composed of three layers: aluminum, polyester, aluminum. The thickness of the window is exaggerated for clarity.

Calculation of the detector efficiency. A schematic diagram of the gas proportional counter used in these experiments is shown in Figure 3 (the thickness of the window is exaggerated for clarity). The radius of the planchet is r_1; the radius of the entrance window is r_2. The height of the planchet wall is h_1; the distance from the bottom of the planchet to the entrance window is h_2. The type of calculation used to determine the efficiency of a particular radionuclide is called a Monte-Carlo simulation. It is assumed that the radionuclide of interest is uniformly distributed throughout the volume of the solid film. Thus, a given decay of a radionuclide atom is equally likely to come from anywhere within the volume of the solid film. In this kind of calculation, the three coordinates of a point in the solid film are chosen at random, using a random number generator, to locate the position of an atom that will decay. The trajectory of the emitted alpha particle can be fixed using two angles in a spherical polar coordinate system. Since the alpha particle

is equally likely to be emitted in any direction, a random number generator is used to assign values to these two angles. (Actually, if one assigns random numbers to the two polar coordinates, one finds that the trajectories tend to be concentrated along the polar axis. To avoid this situation one must weight the random numbers in such a way that the trajectories are truly random. Similar remarks hold for randomly assigning numbers to the coordinates of an atom in the solid film.) Once the position of the decaying radionuclide atom and the direction of the alpha particle have been determined, simple geometric considerations allow one to determine whether the trajectory of the alpha particle intersects the active region of the detector. One must further determine whether the alpha particle can actually reach the active region of the detector before it dissipates all of its energy. This is readily done using the range-energy relationships for alpha particles in the various media. Such range-energy data can be downloaded from the National Institute of Standards ASTAR database.[i] Thus, it can be determined whether the alpha particle arrives in the active region of the detector with sufficient energy to cause a pulse. This step is repeated numerous times. Then the efficiency of a given radionuclide is obtained from the following simple formula:

$$\text{detector efficiency for radionuclide} = \frac{\text{number of alpha particles that reach the active region of the detector}}{\text{number of alpha particles emitted from within the solid film}}$$

In practice, before the gross alpha of a sample is measured, the efficiency of a calibration standard for a range of film masses is determined first. The comparison between the Monte-Carlo simulation and the actual calibration curve is discussed in the next section.

Comparisons between actual calibration curves and calculated calibration curves. Experimental and theoretical plots of calibration curves for Th-230 are shown in Figure 4. The plot through the square symbols (!) is the experimental plot. The plot through the triangular symbols (4) is an theoretical plot in which it is assumed that the solid film is of uniform thickness and that none of the film resides on the wall of the planchet. It is seen that the theoretical plot exceeds the experimental plot by about 0.08. Visual inspection of the solid films in the planchet clearly demonstrates that some of the film resides on the wall of the planchet. In the plot through the round symbols ()) it is assumed that the film is of uniform thickness and that 30% of the film resides on the planchet wall. In this case the theoretical efficiency still exceeds the experimental efficiency by about 0.055. Visual inspection of the solid films clearly demonstrates that they are not of uniform thickness across the planchet. In the plot through the diamond-shaped symbols (э) it is assumed that 30% of the film resides on the wall of the planchet and that the film only covers about 50% of the planchet. That is, the film tends to gather into regions that are relatively thick separated by areas devoid of film. The thick regions cover 50% of the planchet. In this case there is still a substantial discrepancy between the experimental and theoretical calibration curves, especially at low film masses. However, the agreement between the two curves improves as the film mass increases.

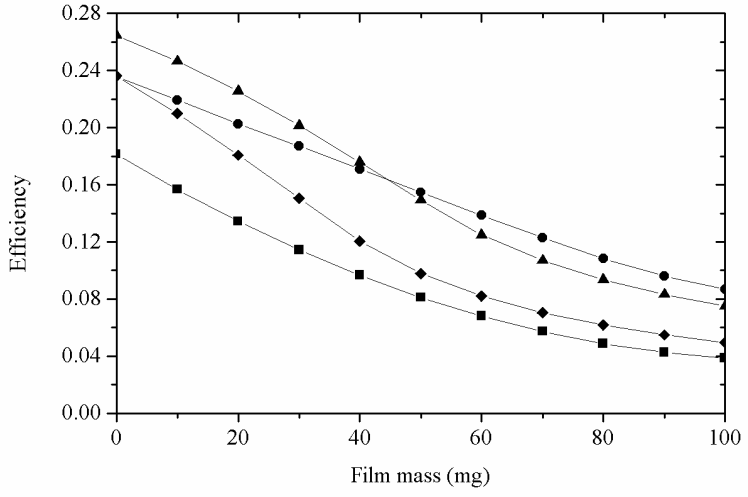

Figure 4. Plot of detector efficiency versus film mass. (!) Experimental calibration curve using Th-230. (4) Simulated calibration curve for Th-230. The film is assumed to be uniform and it is assumed that none of the film is on the wall of the planchet. (0) Simulated calibration curve for Th-230. The film is assumed to be uniform and it is assumed that 30% of the film is on the wall of the planchet. (9)Simulated calibration curve for Th-230. The film is assumed to cover 50% of the planchet and it is assumed that 30% of the film is on the wall of the planchet.

The disparity in efficiency between the calculated calibration curves and the actual calibration curves could be due to any of several factors. First, in the model it is assumed that every alpha particle that enters the active region of the detector with an energy exceeding a certain threshold value causes a pulse in the detector, independent of where the alpha particle enters the active region of the detector. It may be that an alpha particle that enters the detector near one of the anode wires (each detector has two) has a higher probability of causing a pulse than an alpha particle that enters the active region of the detector at some distance from either of the anode wires. It may be necessary to alter the model such that the probability that an alpha particle causes a pulse in the detector declines with its distance from the anode wires. Some library research will be done to determine whether this is the case.

Second, the present Monte-Carlo model does not fully account for the scattering of an alpha particle. The only way in which the present model accounts for scattering is by using the projected range of an alpha particle in the calculations rather than the actual range of the alpha particle. The projected range is the distance that an alpha particle travels from its point of origin; the actual range is the total length of the alpha particle trajectory before it the alpha particle comes to a stop. For practical purposes, alpha particles lose all of their energy in collisions with electrons, collisions with nuclei being exceedingly rare. Since an alpha particle is so much more massive than an electron, the path of the alpha particle deviates by a negligible amount upon colliding with a single electron. However, since the alpha particle undergoes thousands of collisions with electrons, its path, near the end of its travel, may deviate appreciably from its original path. If alpha particles traveled in straight lines, then all alpha particles originating from a given point within the solid film that are emitted within a certain cone with apex at the point of origin and axis perpendicular to the entrance window would reach the active region of the detector and cause a pulse in the detector. Call this cone the emission cone. The emission cone is illustrated in Figure 4. When trajectories lie outside of the emission cone, an alpha particle traveling in a straight line traverses too much matter to reach the active region of the detector. In the Monte-Carlo model used above it is implicitly assumed that an alpha particle may be scattered but that the scattering averages in such a way that the scattered alpha particle does not deviate appreciably from its original direction. This assumption may be the reason for the discrepancy between the calculated results and the experimental results. In this case the model would have to be modified to take into account the angular dispersion in the trajectory of the alpha particles.

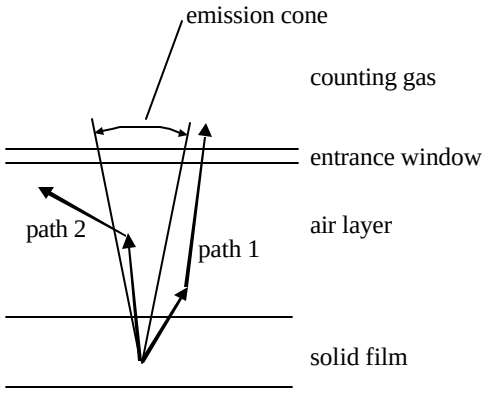

Figure 5. Scattering of an emitted alpha particle. Path 1 shows the trajectory of an alpha particle whose initial trajectory is outside of the emission cone but whose trajectory, upon scattering, takes the alpha particle into the active region of the detector. Path 2 shows the

trajectory of an alpha particle whose initial trajectory is inside the emission cone but whose trajectory, upon scattering, ends before the active region of the detector is reached.

Third, it is not known exactly how the calibration standard is distributed on the planchet, especially when the mass of the film is negligible. Under these conditions there is no visual evidence for how the film is distributed. Some studies will be performed in which the calibration standard is carefully placed on the planchet to assure that the distribution of the standard is known. Such studies should allow one to determine how the efficiency varies with position on the planchet and whether the distribution of the calibration standard on the planchet is responsible for the discrepancy between the experimental and the calculated results.

Conclusion. It is clear that water samples containing Ra-228 must also contain some Ra-224. To a first approximation, it is assumed that the activity of the Ra-224 is equal to the activity of the Ra-228. In addition, both Ra-224 and Ra-226 decay into a series of radioactive progeny, some of which emit alpha particles. The contribution of these progeny to the total alpha activity of the solid film is readily determined using the Bateman equations, once the activities of Ra-224 and Ra-228 are known. Finally, in order that the gross alpha activity be correlated with the activity of the radionuclides in the solid film, it is necessary to develop a model that can be used to calculate the detector efficiency of each radionuclide. Such a model has been developed but needs some modification to more closely approximate the detector efficiencies of the various radionuclides. At this point it seems prudent to proceed with the analyses of the remaining water samples in the study; the modification of the model can be done simultaneously. The appendix gives some results for the water samples analyzed so far.

Appendix. The table below gives some results for the groundwater samples analyzed thus far. Although the samples were analyzed for isotopic thorium and Po-210, these results are not included since, in most cases, the activities of these radionuclides in the samples are negligible.

Table. Activity data for the samples analyzed thus far.

				Gross Alpha	U-234	U-235	U-238	Ra-226	Ra-228
sample ID	location	PWSID	Well no.	Activity (pC/L)	Activity (pC/L)	Activity (pC/L)	Activity (pC/L)	Activity (pC/L)	Activity (pC/L)
78109	Lake Mills		6	11	1.609	0.013	0.312	1.87	2.1
78110	Johnson Creek		2	13	1.367	0.023	0.203	2.08	1.5
78111	Johnson Creek		3	22	0.291	0.006	0.036	4.5	3.6
78112	Lake Mills		5	14	2.298	0.012	0.209	3.0	1.8
78113	Lake Mills		4	13	2.437	0.019	0.318	1.2	1.1
78147	Hustiford Waterworks	11401489	2	19	0.811	0.007	0.090	3.7	3.8
78148	Hustiford Waterworks	11401489	3	40	1.265	0.006	0.301	7.1	6.7
78149	Reeseville Waterworks	11401533	1	5	1.633	0.010	0.207	0.92	0.5
78150	Reeseville Waterworks	11401533	2	22	3.079	0.018	0.457	4.4	2.5
78173	Pell Lake Sanitary District No. 1	26514697	1	64	0.104	0.002	0.016	13.5	7.7
78174	Country Estates Community Assoc.	26501277	4	15	0.041	0.002	0.015	3.0	1.8
78175	Union Grove Waterworks	25202001	4	30	2.471	0.020	0.167	5.8	3.2
78176	Union Grove Waterworks	25202001	5	23	2.400	0.008	0.183	3.7	2.1
78177	Southern Wisconsin Center	25201990	3	29	2.055	0.013	0.159	3.9	3.1
78178	Waterford Waterworks	25202023	2	34	2.499	0.007	0.216	7.1	3.1
78254	Winneconne Waterworks	47103540	1	48	15.691	0.092	1.830	5.5	4.3
78255	Winneconne Waterworks	47103540	2	30	10.288	0.075	1.236	2.34	2.1
78256	Berlin Waterworks	42402162	4	24	2.050	0.019	0.318	2.9	3.1
78257	Berlin Waterworks	42402162	5	20	1.611	0.016	0.231	2.29	2.5
78258	Berlin Waterworks	42402162	6	18	4.615	0.036	0.691	2.80	1.4

78259	Princeton Waterworks	42402195	1	33	1.621	0.012	0.227	5.1	4.1
78260	Princeton Waterworks	42402195	2	28	1.924	0.017	0.313	5.6	3.8
78319	Bellevue TN Sanitary District No. 1	40504596	1	39	4.864	0.026	0.323	8.6	6.0
78320	Bellevue TN Sanitary District No. 1	40504596	2	36	4.472	0.019	0.279	7.4	4.9
78321	Bellevue TN Sanitary District No. 1	40504596	3	66	6.338	0.027	0.328	15.2	5.3
78322	Bellevue TN Sanitary District No. 1	40504596	4	68	5.211	0.028	0.425	17.0	9.0
78323	Allouez Waterworks	40504552	1	21	3.639	0.012	0.206	5.1	3.4
78324	Allouez Waterworks	40504552	2	18	2.183	0.015	0.116	3.7	3.1
78325	Allouez Waterworks	40504552	5	13	2.284	0.007	0.110	2.3	2.2
78326	Allouez Waterworks	40504552	6	44	3.638	0.013	0.188	9.2	4.6
78327	Allouez Waterworks	40504552	7	51	4.529	0.021	0.232	9.3	4.5
79933	Waukesha Water Utility	26802380	9	19	1.1657	0.0169	0.1471	4.9	18.1
79934	Waukesha Water Utility	26802380	8	11	1.0296	0.0080	0.0781	3.2	10
79935	Waukesha Water Utility	26802380	7	9	0.7762	0.0057	0.0683	2.8	4.5
79936	Waukesha Water Utility	26802380	6	13	0.9699	0.0176	0.0855	3.6	16
79937	Waukesha Water Utility	26802380	5	12	2.0085	0.0157	0.1275	3.2	8.4
79938	Waukesha Water Utility	26802380	10	26	1.9587	0.0098	0.1118	5.7	8.4
79939	City of Pewaukee Water & Sewer Utility	26802380	1	17	2.4171	0.0147	0.1740	2.3	3.8
79940	City of Pewaukee Water & Sewer Utility	26802380	2	22	1.5326	0.0074	0.1378	5.4	3.4
79941	City of Pewaukee Water & Sewer Utility	26802380	5	12	5.5356	0.0422	0.6831	1.93	1.5
79942	City of Pewaukee Water & Sewer Utility	26802380	6	11	2.9032	0.0173	0.2593	2.8	2.5
80348	Squires Grove	26802017	2	53	5.6591	0.0182	0.1272	8.5	5.0
80349	New Berlin Water Utility	26802171	1	26	3.7445	0.0189	0.1597	4.2	3.3
80350	New Berlin Water Utility	26802171	3	27	3.8485	0.0155	0.1926	4.0	3.8
80351	New Berlin Water Utility	26802171	4	20	3.7973	0.0151	0.1435	3.5	3.7
80352	New Berlin Water Utility	26802171	7	42	2.8358	0.0185	0.1579	3.8	3.8
80353	New Berlin Water Utility	26802171	8	49	4.0503	0.0309	0.2086	5.4	19.8
80354	Brookfield Water Utility	26802534	6	1	0.2903	0.0090	0.2269	0.39	0.7
80355	Brookfield Water Utility	26802534	15	27	4.4401	0.0156	0.1831	4.5	2.8
80356	Brookfield Water Utility	26802534	22	18	3.4231	0.0132	0.1099	3.0	2.9
80357	Brookfield Water Utility	26802534	29	28	2.7714	0.0131	0.0931	1.85	2.8
80507	Menomonee Falls		7	45	2.4363	0.0167	0.0815	2.9	4.2
80508	Mukwonago		3	19	0.6165	0.0167	0.0434	3.7	3.0
80509	Muskego		2	34	3.5760	0.0054	0.1888	5.6	4.9
80510	Eagle		1	35	0.1090	0.0186	0.0159	5.2	3.5
80511	Menomonee Falls		3	96	6.2995	0.0185	0.2065	5.4	12
80512	Mukwonago		4	34	1.7695	0.0309	0.0942	5.8	5.3
80513	Eagle		2	29	0.1253	0.0090	-0.0012	5.89	3.73
80514	Hales Corners		1	55	4.2799	0.0156	0.1911	6.28	3.99
80515	Menomonee Falls		5	75	6.1653	0.0132	0.2720	6.74	8.59
80516	Hales Corners-Lake Lore			38	2.5499	0.0123	0.1324	4.20	3.86
80730	Gresham Waterworks	45904540	1	11	3.1055	0.0793	2.1090	0.65	0.95
80731	Gresham Waterworks	45904540	2	32	17.2857	0.2583	5.7308	0.64	1.15
80732	Gresham Waterworks	45904540	3	183	82.7416	1.1239	24.2643	0.59	0.21
80733	Kaukauna Electric and Water Dept.	44503360	4	78	2.1372	0.0049	0.1251	3.26	4.58
80734	Kaukauna Electric and Water Dept.	44503360	5	53	2.2714	0.0147	0.1502	2.96	3.37
80735	Kaukauna Electric and Water Dept.	44503300	10	37	1.6509	0.0090	0.1242	3.06	2.71

80736	Shawano Municipal Utilities	45904562	2	78	63.1130	0.7312	16.2308	1.12	1.26
80737	Shawano Municipal Utilities	45904562	3	62	42.6959	0.5342	10.6856	0.94	0.56
80742	Thorp Waterworks	61003371	9	24.8	2.0375	0.0304	0.6186	0.89	2.19
80743	Thorp Waterworks	61003371	12	143.8	78.2067	1.1542	25.3231	3.54	1.43

[i] This data can be downloaded from web site http://physics.nist.gov/PhysRefData /Star/Text/ ASTAR. html.